

# The spin structure of the pion

D. Brömmel,<sup>1,2</sup> M. Diehl,<sup>1</sup> M. Göckeler,<sup>2</sup> Ph. Hägler,<sup>3</sup> R. Horsley,<sup>4</sup> Y. Nakamura,<sup>5</sup>  
D. Pleiter,<sup>5</sup> P.E.L. Rakow,<sup>6</sup> A. Schäfer,<sup>2</sup> G. Schierholz,<sup>1,5</sup> H. Stüben,<sup>7</sup> and J.M. Zanotti<sup>4</sup>

(QCDSF/UKQCD Collaborations)

<sup>1</sup>Deutsches Elektronen-Synchrotron DESY, 22603 Hamburg, Germany

<sup>2</sup>Institut für Theoretische Physik, Universität Regensburg, 93040 Regensburg, Germany

<sup>3</sup>Institut für Theoretische Physik T39, Physik-Department der TU München,  
James-Frank-Straße, 85747 Garching, Germany\*

<sup>4</sup>School of Physics, University of Edinburgh, Edinburgh EH9 3JZ, UK

<sup>5</sup>John von Neumann-Institut für Computing NIC / DESY, 15738 Zeuthen, Germany

<sup>6</sup>Theoretical Physics Division, Department of Mathematical Sciences,  
University of Liverpool, Liverpool L69 3BX, UK

<sup>7</sup>Konrad-Zuse-Zentrum für Informationstechnik Berlin, 14195 Berlin, Germany

(Dated: June 3, 2019)

We present the first calculation of the transverse spin structure of the pion in lattice QCD. We find a characteristic asymmetry in the spatial distribution of transversely polarized quarks. This asymmetry is very similar in magnitude to the analogous asymmetry we previously obtained for quarks in the nucleon. Our results support the hypothesis that all Boer-Mulders functions are alike.

*Introduction.*— Since their discovery in the late 1940s, pions have played a central role in low- and high-energy nuclear and particle physics. As pseudo-Goldstone bosons of spontaneously broken chiral symmetry they are at the core of the low-energy sector of quantum chromodynamics (QCD), the fundamental theory of quarks and gluons. Since the pion has spin zero, one might expect that its spin structure in terms of quark and gluon degrees of freedom is trivial. Indeed, pion matrix elements of quark and gluon helicity operators vanish due to parity invariance, i.e., one has  $\langle \pi(P') | \Sigma^3 | \pi(P) \rangle = 0$ , where, e.g., for quarks  $\Sigma^3 = \bar{q} \gamma^3 \gamma_5 q$ .

An instructive quantity describing the spin structure of hadrons is the probability density  $\rho(x, b_\perp)$  of quarks in impact parameter space [1], illustrated in Fig. 1. Here  $x$  is the longitudinal momentum fraction carried by the quark, and the impact parameter  $b_\perp$  gives the distance between the quark and the center of momentum of the hadron in the plane transverse to its longitudinal motion. Because matrix elements of axial-vector operators vanish for the pion, the density  $\rho(x, b_\perp, \lambda)$  of quarks with helicity  $\lambda$  is determined by the unpolarized density,  $2\rho(x, b_\perp, \lambda) = \rho(x, b_\perp)$ . The latter, in turn, is given by the impact parameter dependent generalized quark distribution  $H^\pi(x, \xi, b_\perp^2)$  (see, e.g., [2]) at zero skewness  $\xi$ , i.e.,  $\rho(x, b_\perp) = H^\pi(x, \xi=0, b_\perp^2)$ . The lattice QCD calculations discussed below give access to  $x$ -moments of quark spin densities, which we have investigated in [3] for the case of quarks with transverse spin  $s_\perp$  in a nucleon

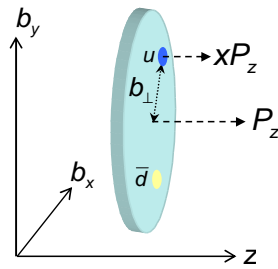


FIG. 1: Illustration of the quark distribution in a  $\pi^+$  in impact parameter space.

with transverse spin  $S_\perp$ . The corresponding expression  $\rho(x, b_\perp, s_\perp)$  for polarized quarks in the pion is readily obtained by setting  $S_\perp = 0$  in the nucleon densities of [3, 4]. The result is considerably simpler but still contains a dipole term going with  $s_\perp^i \epsilon^{ij} b_\perp^j$ , which leads to a dependence on the direction of  $b_\perp$  for fixed  $s_\perp$ ,

$$\rho^n(b_\perp, s_\perp) = \int_{-1}^1 dx x^{n-1} \rho(x, b_\perp, s_\perp) = \frac{1}{2} \left[ A_{n0}^\pi(b_\perp^2) - \frac{s_\perp^i \epsilon^{ij} b_\perp^j}{m_\pi} \frac{\partial}{\partial b_\perp^2} B_{Tn0}^\pi(b_\perp^2) \right]. \quad (1)$$

The  $b_\perp$  dependent vector and tensor generalized form factors (GFFs) of the pion,  $A_{n0}^\pi$  and  $B_{Tn0}^\pi$ , are moments of the corresponding generalized parton distributions (GPDs)

$$\int_{-1}^1 dx x^{n-1} H^\pi(x, \xi=0, b_\perp^2) = A_{n0}^\pi(b_\perp^2), \quad \int_{-1}^1 dx x^{n-1} E_T^\pi(x, \xi=0, b_\perp^2) = B_{Tn0}^\pi(b_\perp^2). \quad (2)$$

To this day, next to nothing is known about the signs and sizes of the  $B_{Tn0}^\pi$ . Since these GFFs determine the dipole-like distortion of the quark density in the transverse plane, non-vanishing  $B_{Tn0}^\pi$  would imply a rather surprising *non-trivial transverse spin structure of the pion*. A computation of the  $B_{Tn0}^\pi$  from first principles in lattice QCD therefore provides crucial insight into the pion structure.

Lattice QCD calculations give access to GFFs  $F(t) = A_{n0}^\pi(t), B_{Tn0}^\pi(t)$  in momentum space, which are related to the impact parameter dependent GFFs  $F(b_\perp^2) = A_{n0}^\pi(b_\perp^2), B_{Tn0}^\pi(b_\perp^2)$  by a Fourier transformation

$$F(b_\perp^2) = (2\pi)^{-2} \int d^2 \Delta_\perp e^{-ib_\perp \cdot \Delta_\perp} F(t = -\Delta_\perp^2), \quad (3)$$

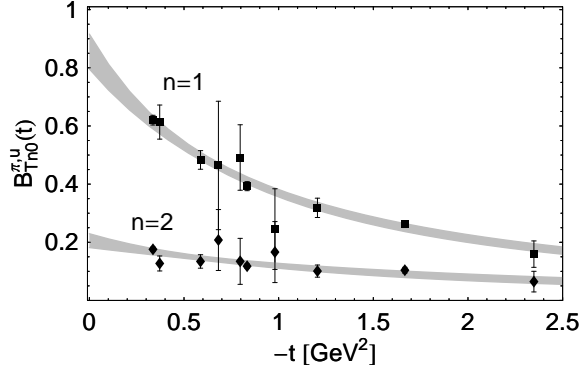


FIG. 2: Lattice results at  $\beta = 5.29$  and  $m_\pi \approx 600$  MeV for the first two generalized form factors  $B_{Tn0}^{\pi,u}(t)$  for up-quarks in the  $\pi^+$  as functions of the invariant momentum transfer  $t$ . The corresponding  $p$ -pole parameterizations are shown by the shaded bands.

where  $\Delta_\perp$  is the transverse momentum transfer. The momentum-space GFFs  $B_{Tn0}^{\pi,u}(t)$  parameterize pion matrix elements of local tensor quark operators,

$$\langle \pi^+(P') | \mathcal{O}_T^{\mu\nu\mu_1\cdots\mu_{n-1}} | \pi^+(P) \rangle = \mathcal{A}S \frac{\bar{P}^\mu \Delta^\nu - \Delta^\mu \bar{P}^\nu}{m_\pi} \times \sum_{\substack{i=0 \\ \text{even}}}^{n-1} \Delta^{\mu_1} \cdots \Delta^{\mu_i} \bar{P}^{\mu_{i+1}} \cdots \bar{P}^{\mu_{n-1}} B_{Tni}^{\pi,u}(t) \quad (4)$$

with  $\bar{P} = \frac{1}{2}(P' + P)$ ,  $\Delta = P' - P$  and  $t = \Delta^2$ . Here  $\mathcal{A}S$  denotes symmetrization in  $\nu, \dots, \mu_{n-1}$  followed by anti-symmetrization in  $\mu, \nu$  and subtraction of traces in all index pairs. The tensor operators are given by

$$\mathcal{O}_T^{\mu\nu\mu_1\cdots\mu_{n-1}} = \mathcal{A}S \bar{q} i\sigma^{\mu\nu} i\overleftrightarrow{D}^{\mu_1} \cdots i\overleftrightarrow{D}^{\mu_{n-1}} q \quad (5)$$

with  $\overleftrightarrow{D} = \frac{1}{2}(\vec{D} - \overleftarrow{D})$  and all fields taken at space-time point  $z = 0$ . The analogous matrix elements of local vector quark operators are parameterized by  $A_{n0}^{\pi,u}(t)$  as specified in [5]. For definiteness we consider in the following the GFFs  $A_{n0}^{\pi,u}(t)$  and  $B_{Tn0}^{\pi,u}(t)$  for up-quarks in a  $\pi^+$ . Their counterparts for down-quarks and for  $\pi^-$  or  $\pi^0$  can be easily determined by charge conjugation and isospin invariance [2], since Wilson fermions preserve flavor symmetry. We note that  $A_{10}^{\pi,u}(t)$  is identical to the electromagnetic pion form factor  $F_\pi(t)$ , which we investigated in detail in [6].

*Lattice QCD results.*— State-of-the-art lattice calculations allow us to evaluate the matrix elements in Eq. (4) for  $n = 1, 2$  and momentum transfers up to  $-t \approx 3$  GeV<sup>2</sup>. Our simulations are based on Wilson gluons and dynamical, non-perturbatively  $\mathcal{O}(a)$  improved Wilson fermions with  $n_f = 2$ . Configurations have been generated at four different couplings  $\beta = 5.20, 5.25, 5.29, 5.40$  with up to five different  $\kappa = \kappa_{\text{sea}}$  values per  $\beta$ , on lattices of sizes  $V \times T = 16^3 \times 32$  and  $24^3 \times 48$ . We have set the lattice scale  $a$  using a Sommer parameter of  $r_0 = 0.467$  fm [7, 8].

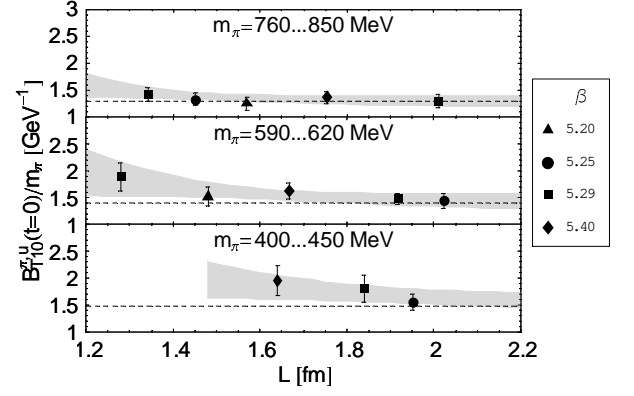


FIG. 3: Study of finite size effects of  $B_{T10}^{\pi,u}(t=0)/m_\pi$  for three different ranges of pion masses. Shaded bands (restricted to the region  $m_\pi L > 3$ ) represent estimates of the volume dependence based on a combined fit in  $m_\pi$  and  $L$  as described in the text. The dashed lines show the infinite-volume limit of the fit at the corresponding average pion mass.

The pion masses are as low as 400 MeV, spatial volumes are as large as  $(2.1 \text{ fm})^3$ , and lattice spacings are below 0.1 fm. Details on the lattice parameters are given in [6]. The computationally demanding disconnected contributions present for even  $n$  are not included. For the tensor GFFs  $B_{Tn0}^{\pi,u}$  we expect them to be small in the physical limit, since they require a chirality flip on a quark line and are thus suppressed by the quark mass [9]. The lattice results have been transformed to the  $\overline{\text{MS}}$  scheme at a scale of 4 GeV<sup>2</sup> using non-perturbative renormalization [10]. Further information on the procedures to compute GFFs in lattice QCD can be found, e.g., in [6, 11, 12], and details of the present analysis will be given in [13].

As an example we show in Fig. 2 the  $t$  dependence of the GFFs  $B_{Tn0}^{\pi,u}(t)$  for  $n = 1, 2$  at  $\beta = 5.29$  and a pion mass of  $m_\pi \approx 600$  MeV. The extrapolation to the forward limit  $t = 0$  requires a parameterization of the  $t$  dependence of the lattice results, which is obtained from a fit to a  $p$ -pole form  $F(t) = F_0/[1 - t/(pm_p^2)]^p$ , where the forward value  $F_0 = F(t=0)$ , the  $p$ -pole mass  $m_p$ , and the power  $p$  are free parameters for each GFF. The statistics and  $t$  range of our data are not sufficient to determine the powers  $p$  in the fits. To avoid divergent densities at  $b_\perp = 0$  in impact parameter space, we restrict the powers to  $p > 1$  for  $A_{n0}^{\pi,u}(t)$  and to  $p > 3/2$  for  $B_{Tn0}^{\pi,u}(t)$  according to [4]. Since our fits indicate that in general smaller values of  $p$  are preferred, we set in the following  $p = 1.1$  for  $A_{n0}^{\pi,u}(t)$  and  $p = 1.6$  for  $B_{Tn0}^{\pi,u}(t)$ . As we cannot resolve structures at arbitrarily small distances, these powers should be considered as effective values suitable for the range of momenta accessible in our simulation. Taking  $p = 2$ , which corresponds to the behavior expected for  $-t \rightarrow \infty$ , changes the results for  $B_{T(n=1,2)0}^{\pi,u}(t=0)$  by less than the statistical error. For the examples in Fig. 2 our fits give  $B_{T10}^{\pi,u}(t=0) = 0.856(60)$  with  $m_p = 0.949(57)$  GeV for the first moment, and  $B_{T20}^{\pi,u}(t=0) = 0.206(24)$  with

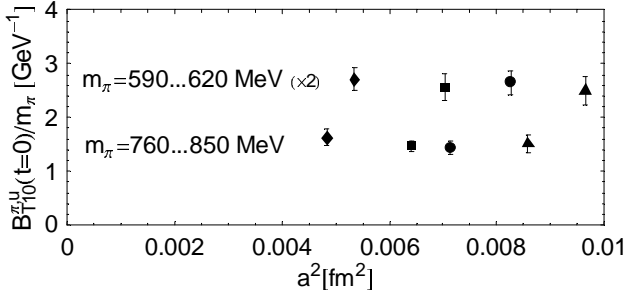


FIG. 4: Study of discretization errors in  $B_{T10}^{\pi,u}(t=0)/m_{\pi}$ . The symbols are as in Fig. 3.

$m_p = 1.239(30)$  GeV for the second moment.

Before discussing potential finite size and discretization effects as well as the pion mass dependence of our results we note that, due to the prefactor  $m_{\pi}^{-1}$  in the parameterization (4), the GFFs  $B_{Tn0}^{\pi}(t)$  must vanish like  $m_{\pi}$  for  $m_{\pi} \rightarrow 0$  [2]. This is also required to ensure that the densities in Eq. (1) stay positive and finite in the chiral limit. In the following we therefore consider the ratio  $B_{Tn0}^{\pi}/m_{\pi}$ , which tends to a constant at  $m_{\pi} = 0$ .

Figure 3 shows the volume dependence of the forward value  $B_{T10}^{\pi,u}(t=0)/m_{\pi}$  for three different ranges of pion masses. The finite volume corrections to the matrix elements with  $n = 1, 2$  in Eq. (4) are known to leading order in chiral perturbation theory (ChPT) [14]. For  $m_{\pi}L \gg 1$  the leading correction to  $B_{Tn0}^{\pi}(t=0)/m_{\pi}$  is proportional to  $m_{\pi}^2 \exp(-m_{\pi}L)$  up to powers of  $(m_{\pi}L)^{-1/2}$ , where  $L$  is the spatial extent of the lattice. Although our analysis includes pion masses as low as 400 MeV, we feel that a quantitative application of the chiral expansion requires lattice computations at even lower values of  $m_{\pi}$  and probably the inclusion of higher-order terms. We take however the result of [14] as a guide to estimate the  $L$  dependence of our lattice data, fitting  $B_{T10}^{\pi,u}(t=0)/m_{\pi}$  to the form  $c_0 + c_1 m_{\pi}^2 + c_2 m_{\pi}^2 \exp(-m_{\pi}L)$ . This fit, represented by the shaded bands in Fig. 3, suggests that  $[B_{T10}^{\pi,u}(t=0)/m_{\pi}]_L > [B_{T10}^{\pi,u}(t=0)/m_{\pi}]_{L \rightarrow \infty}$ . For  $B_{T20}^{\pi,u}(t=0)/m_{\pi}$  the situation is similar. Within present statistics, we do not see a clear volume dependence of the corresponding  $p$ -pole masses for  $n = 1, 2$ .

Figure 4 shows the dependence of  $B_{T10}^{\pi,u}(t=0)/m_{\pi}$  on the lattice spacing  $a$  for two ranges of pion masses, where we have excluded those lattice data points which are most strongly affected by finite volume corrections. We conclude that discretization errors are smaller than the statistical errors and neglect any dependence of the GFFs on  $a$  in the following analysis.

The pion mass dependence of the forward values  $B_{Tn0}^{\pi,u}(t=0)/m_{\pi}$  is shown in Fig. 5. Following our above remarks we do not attempt to fit this dependence to the one-loop result of ChPT [2, 14], and limit ourselves to a linear extrapolation in  $m_{\pi}^2$  of the forward values and the squared  $p$ -pole masses. The resulting fits are shown in the figure as shaded bands. For  $m_{\pi} = 140$  MeV we ob-

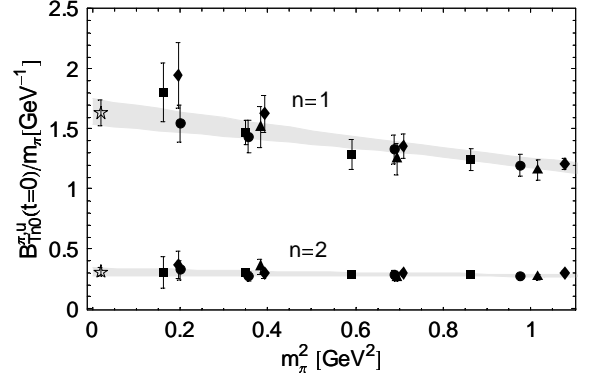


FIG. 5: Pion mass dependence of  $B_{Tn0}^{\pi,u}(t=0)/m_{\pi}$ . The shaded bands represent a fit linear in  $m_{\pi}^2$ , and the stars give the corresponding values extrapolated to the physical point. The symbols are as in Fig. 3.

tain  $B_{T10}^{\pi,u}(t=0)/m_{\pi} = 1.64 \pm 0.11$  (stat)  $- 0.33$  (vol)  $\text{GeV}^{-1}$  with a  $p$ -pole mass of  $m_p = 0.732 \pm 0.095$  GeV, and  $B_{T20}^{\pi,u}(t=0)/m_{\pi} = 0.307 \pm 0.032$  (stat)  $- 0.06$  (vol)  $\text{GeV}^{-1}$  with  $m_p = 0.938 \pm 0.260$  GeV, where in both cases we have set  $p = 1.6$  and included an estimated 20% uncertainty for finite volume effects in the forward values.

To compute the lowest two moments of the density in Eq. (1) we need in addition the GFFs  $A_{n0}^{\pi}(t)$  with  $n = 1, 2$ . For  $A_{10}^{\pi,u}(t) = F_{\pi}(t)$  we refer to our results in [6]. A detailed analysis of  $A_{20}^{\pi,u}(t)$  will be presented in [13], and first results can be found in [5]. For the evaluation of the densities  $\rho^n(b_{\perp}, s_{\perp})$  we Fourier transform the  $p$ -pole parameterizations of the momentum-space GFFs. In Fig. 6 we show the lowest two moments of the density for up-quarks in a  $\pi^+$ . Compared to the unpolarized case on the left, we find substantial distortions on the right-hand side of Fig. 6 for transversely polarized quarks and thus a pronounced spin structure. From Eq. (1) we readily obtain an average transverse shift

$$\langle b_{\perp}^y \rangle_n = \frac{\int d^2 b_{\perp} b_{\perp}^y \rho^n(b_{\perp}, s_{\perp})}{\int d^2 b_{\perp} \rho^n(b_{\perp}, s_{\perp})} = \frac{1}{2m_{\pi}} \frac{B_{Tn0}^{\pi,u}(t=0)}{A_{n0}^{\pi,u}(t=0)} \quad (6)$$

in the  $y$  direction for transverse quark spin  $s_{\perp} = (1, 0)$  in the  $x$  direction. Our lattice results give  $\langle b_{\perp}^y \rangle_1 = 0.162(11)$  fm and  $\langle b_{\perp}^y \rangle_2 = 0.117(13)$  fm, where we quote only statistical errors.

Let us compare our results for  $B_{Tn0}^{\pi}$  with those for the analogous GFFs  $\overline{B}_{Tn0}$  that describe the dipole-like distortion in the density of transversely polarized quarks in an unpolarized nucleon. The corresponding average transverse shift is  $\langle b_{\perp}^y \rangle_n = \overline{B}_{Tn0}(t=0)/(2m_N A_{n0}(t=0))$ , where  $A_{n0}(t=0)$  is a moment of the unpolarized quark distribution. With the lattice results of [3] we find  $\langle b_{\perp}^y \rangle_1 = 0.154(6)$  fm and  $\langle b_{\perp}^y \rangle_2 = 0.101(8)$  fm for up-quarks in the proton. Remarkably, the distortion in the distribution of a transversely polarized up-quark is within errors of the same strength in a  $\pi^+$  and in the proton.

The moments of the GPDs  $E_T^{\pi}$  in the pion and  $\overline{E}_T$  in

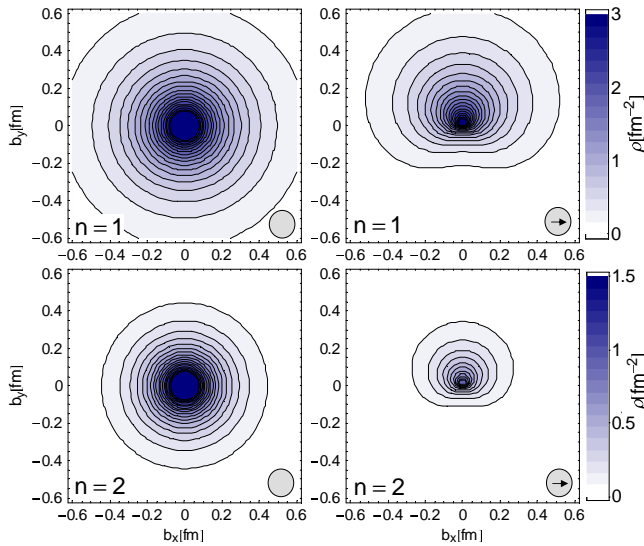


FIG. 6: The lowest two moments of the impact parameter densities of unpolarized (left) and transversely polarized (right) up-quarks in a  $\pi^+$ . The quark spin (inner arrow) is oriented in the transverse plane as indicated.

the nucleon can be connected with the respective Boer-Mulders functions, which describe the correlation between transverse spin and intrinsic transverse momentum of quarks in an unpolarized hadron [15]. They lead, e.g., to azimuthal asymmetries in semi-inclusive deep inelastic scattering (SIDIS) and in Drell-Yan lepton pair production. The density of quarks with intrinsic transverse momentum  $k_\perp$  and transverse spin  $s_\perp$  in a  $\pi^+$  is determined by the unpolarized distribution  $f_1^\pi$  and the Boer-Mulders function  $h_1^{\pi,\perp}$  through

$$f(x, k_\perp, s_\perp) = \frac{1}{2} \left[ f_1^\pi(x, k_\perp^2) + \frac{s_\perp^i \epsilon^{ij} k_\perp^j}{m_\pi} h_1^{\pi,\perp}(x, k_\perp^2) \right]. \quad (7)$$

We notice the close similarity between Eq. (7) and the impact parameter density (1), but emphasize that  $k_\perp$  and  $b_\perp$  are *not* Fourier conjugate variables. A dynamical relation between  $k_\perp$  and  $b_\perp$  dependent distributions has been proposed in [16, 17] and implies  $h_1^{\perp,\pi} \sim -E_T^\pi$ . With Eq. (2) and our results for  $B_{Tn0}^\pi$  we then predict that the Boer-Mulders function for up-quarks in a  $\pi^+$  is large and negative. Furthermore, our comparison of pion and nucleon results provides strong support for the arguments in [18], which suggest that Boer-Mulders functions for valence quarks are negative and of similar size relative to the unpolarized distributions, independent of the hadron under consideration. We note that  $h_1^{\perp,\pi}$  is time reversal odd and thus enters with different sign in SIDIS and Drell-Yan production [19]. The results just quoted refer to the functions relevant for SIDIS.

*Conclusions.*— We have calculated the first two moments of the quark tensor GPD  $E_T^\pi$  in the pion. We find that the spatial distribution of quarks is strongly dis-

torted if they are transversely polarized, which reveals a non-trivial spin structure of the pion. The effect has the same sign and very similar magnitude as the corresponding distortion for quarks in the nucleon [3]. Assuming the relation between impact parameter and transverse momentum densities proposed in [16, 17] this suggests that all Boer-Mulders functions for valence quarks may be alike, as argued in [18]. The large size of the effect might give new insight into the mechanism responsible for the large  $\cos(2\phi)$  azimuthal asymmetry observed in unpolarized  $\pi p$  Drell-Yan production, which is sensitive to the product  $h_1^{\perp,\pi} h_1^\perp$ , see, e.g., the discussion in [20] and references therein. It also provides additional motivation for future studies of azimuthal asymmetries in unpolarized  $\pi p$  and polarized  $\pi p^\dagger$  Drell-Yan production at COMPASS, the latter giving rise to a  $\sin(\phi + \phi_S)$  asymmetry sensitive to  $h_1^{\perp,\pi} h_1^\perp$ , where  $h_1^\perp$  is the quark transversity distribution in the nucleon [21].

The numerical calculations have been performed on the Hitachi SR8000 at LRZ (Munich), apeNEXT and APEmille at NIC/DESY (Zeuthen) and BlueGene/Ls at NIC/FZJ (Jülich), EPCC (Edinburgh) and KEK (by the Kanazawa group as part of the DIK research program). This work was supported by DFG (Forschergruppe Gitter-Hadronen-Phänomenologie and Emmy-Noether program), by HGF (contract No. VH-NG-004) and by EU I3HP (contract No. RII3-CT-2004-506078).

\* Electronic address: phaegler@ph.tum.de

- [1] M. Burkardt, Phys. Rev. D **62**, 071503 (2000) [Erratum ibid. D **66**, 119903 (2002)]; Int. J. Mod. Phys. A **18**, 173 (2003).
- [2] M. Diehl, A. Manashov and A. Schäfer, Phys. Lett. B **622**, 69 (2005).
- [3] M. Göckeler *et al.*, Phys. Rev. Lett. **98**, 222001 (2007).
- [4] M. Diehl and Ph. Hägler, Eur. Phys. J. C **44**, 87 (2005).
- [5] D. Brömmel *et al.*, PoS **LAT2005**, 360 (2006).
- [6] D. Brömmel *et al.*, Eur. Phys. J. C **51**, 335 (2007).
- [7] A. Ali Khan *et al.*, Phys. Rev. D **74**, 094508 (2006).
- [8] C. Aubin *et al.*, Phys. Rev. D **70** (2004) 094505.
- [9] M. Göckeler *et al.*, Phys. Lett. B **627**, 113 (2005).
- [10] G. Martinelli *et al.*, Nucl. Phys. B **445**, 81 (1995); M. Göckeler *et al.*, Nucl. Phys. B **544**, (1999) 699.
- [11] M. Göckeler *et al.*, Phys. Rev. Lett. **92**, 042002 (2004); Nucl. Phys. A **755**, 537 (2005).
- [12] Ph. Hägler *et al.*, Phys. Rev. D **68**, 034505 (2003).
- [13] D. Brömmel *et al.*, in preparation.
- [14] A. Manashov and A. Schäfer, arXiv:0706.3807.
- [15] D. Boer and P. J. Mulders, Phys. Rev. D **57**, 5780 (1998).
- [16] M. Burkardt, Phys. Rev. D **72**, 094020 (2005).
- [17] S. Meissner, A. Metz and K. Goeke, hep-ph/0703176.
- [18] M. Burkardt and B. Hannafious, arXiv:0705.1573.
- [19] J. C. Collins, Phys. Lett. B **536**, 43 (2002).
- [20] D. Boer, Phys. Rev. D **60** (1999) 014012.
- [21] A. Sissakian *et al.*, Eur. Phys. J. C **46**, 147 (2006); A. Bianconi and M. Radici, Phys. Rev. D **73**, 114002 (2006).